

Constant rate shearing on two-dimensional cohesive discs

This article has been downloaded from IOPscience. Please scroll down to see the full text article.

2005 J. Phys.: Condens. Matter 17 5677

(<http://iopscience.iop.org/0953-8984/17/37/006>)

View [the table of contents for this issue](#), or go to the [journal homepage](#) for more

Download details:

IP Address: 129.252.86.83

The article was downloaded on 28/05/2010 at 05:57

Please note that [terms and conditions apply](#).

Constant rate shearing on two-dimensional cohesive discs

N Olivi-Tran¹, O Pozo² and N Fraysse²

¹ SPCTS, UMR-CNRS 6638, Ecole Nationale Supérieure de Céramiques Industrielles, 47 avenue Albert Thomas, 87065 Limoges cedex, France

² LPMC, UMR-CNRS 6622, Parc Valrose, Université de Nice Sophia Antipolis, 06108 Nice cedex 2, France

Received 10 May 2005, in final form 25 July 2005

Published 2 September 2005

Online at stacks.iop.org/JPhysCM/17/5677

Abstract

We performed two-dimensional molecular dynamics simulations of cohesive discs under shear. The cohesion between the discs is added by the action of springs between very next neighbouring discs, modelling capillary forces. The geometry of the cell allows disc–disc shearing and not disc–cell wall shearing as is commonly found in the literature. Does a stick–slip phenomenon happen though the upper cover moves at a constant velocity, i.e. with an infinite shearing force? We measured the forces with which the discs acted on the upper cover for different shearing rates, as well as the disc velocities as a function of the distance to the bottom of the cell. It appears that the forces measured versus time present a periodic behaviour, very close to a stick–slip phenomenon, for shearing rates larger than a given threshold. The discs' collective displacements in the shearing cell (back and ahead) are the counterpart of the constant velocity of the upper cover, leading to a periodic behaviour of the shear stress.

1. Introduction

It frequently happens in nature that a system under continuous driving force responds in an intermittent way. Time intervals when the system is at rest and potential energy is accumulated alternate with active periods, when the system relaxes and potential energy is decreased. Since the simplest interaction leading to such behaviour is friction between two moving objects, these phenomena are called stick–slip processes. Since one of the dominating interactions in granular materials is friction among the grains, it is not surprising that dense granular materials exhibit various stick–slip phenomena.

Cohesion is generally put into a granular system by the mean of a liquid added to the grains. The presence of cohesion adds a new dimension to the underlying physics of granular materials. Experimentally and numerically, the physics of humid granular media only began in the late 1990s [1–11, 14–17].

Here we will study numerically a two-dimensional shearing cell containing mono-disperse cohesive discs. The cohesion in our model is very weak: in comparison, this cohesion may be experimentally obtained by the addition of an undersaturated water vapour atmosphere surrounding spherical beads. Hence, cohesion here is very different from that obtained with addition of macroscopic quantities of liquid. In this cell, the shearing rate is constant, i.e. the shearing driving force is infinite. Thus, the system as a whole cannot be at rest. We will analyse the behaviours of our two-dimensional cohesive discs, and study the shear stress as a function of time, with a molecular dynamics model [14, 15] of the experiment in order to answer the question: does a stick–slip phenomenon happen in cohesive discs dragged with an infinite shearing force?

2. Numerical model

Molecular dynamics is a powerful numerical method to study the dynamics of granular materials [12]. The model we used here is a version of molecular dynamics for granular flow with cohesion in a two-dimensional shearing cell [12–15]. Particles are modelled as N discs that have equal density $d = 2.2 \text{ g cm}^{-2}$ and diameters $d = 0.2 \text{ mm}$.

The only external force acting on the system results from gravity, $g = 981 \text{ cm s}^{-2}$. The particle–particle and particle–wall contacts are described in the normal direction (i.e. in the particles' centre–centre direction) by a Hooke-like force law. The normal force is written

$$\mathbf{f}_n(i, j) = \left(-Y r_{\text{eff}} \left[\frac{1}{2}(d_i + d_j) - |\mathbf{r}_{i,j}| \right] + \gamma \frac{m_{\text{eff}}(\mathbf{v}_{i,j} \cdot \mathbf{r}_{i,j})}{r_{\text{eff}} |\mathbf{r}_{i,j}|} \right) \frac{\mathbf{r}_{i,j}}{|\mathbf{r}_{i,j}|} \quad (1)$$

where Y is the Young modulus of the solid, r_{eff} (m_{eff}) stands for the effective radius (mass) of the particles i and j and $\mathbf{v}_{ij} = \mathbf{v}_i - \mathbf{v}_j$ is the relative velocity of particle j towards particle i . The effective radius is defined here as the radius of a disc which effectively enters into interaction with another disc; it can be smaller than the real disc radius in the case where the discs overlap or larger in the case of capillary interaction (see below). The effective radius is proportional to the distance between the centres of the discs if these two are in interaction. The effective mass is defined here as the mass which contributes to the shearing; in our case all discs have their effective mass equal to their real mass except the discs which build the bottom of the shearing cell. d_i (d_j) is the diameter of particle i (j) and \mathbf{r}_{ij} points from particle i to particle j . γ is a phenomenological dissipation coefficient.

We model the static friction force between particles by putting a virtual spring at the point of first contact. Its elongation is integrated over the entire collision time and set to zero when the contact is lost. The maximum possible value of the restoring force in the shear direction (i.e. in the plane perpendicular to the normal direction), according to Coulomb's criterion, is proportional to the normal force multiplied by the friction coefficient μ . It gives a friction force $\mathbf{f}_s(i, j)$ which is written

$$\mathbf{f}_s(i, j) = -\text{sign}(f_f(i, j)) \min(f_f(i, j), \mu |f_n(i, j)|) \mathbf{s} \quad (2)$$

$$\mathbf{f}_f(i, j) := - \int (\dot{r}_i - \dot{r}_j) \mathbf{s} dt \quad (3)$$

where \mathbf{s} stands for the unit vector in the shear direction. When a particle collides with the cylinder wall, the same forces (1) and (2) act with infinite mass and radius for particle j .

Capillary forces were modelled by adding a spring force to the normal force when particles are in contact:

$$f_{\text{cap}} = K r_{\text{eff}} \frac{1}{2}(d_i + d_j) \quad (4)$$

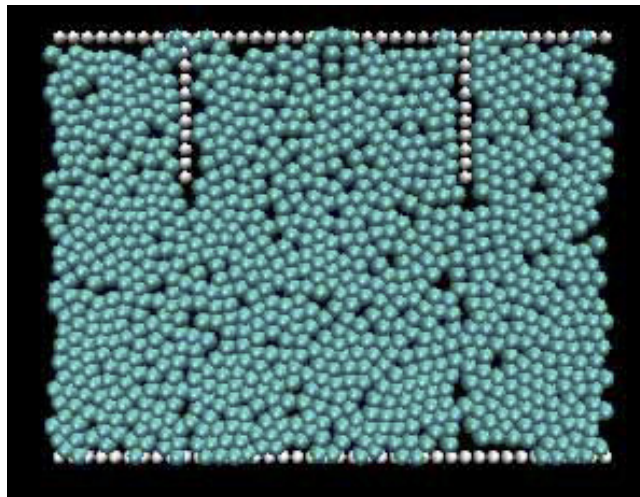


Figure 1. Shearing cell.
(This figure is in colour only in the electronic version)

where K is the corresponding spring constant, which depends on the surface tension and on the viscosity of the liquid. When the distance (proportional to the effective radius) between the surface of the particles is lower than 10% of the diameter of the smallest particle, the value of the spring constant is multiplied by the distance between the particles. This additive force is set to zero when the elongation of the virtual spring reaches a maximum length of 10% of the smallest particle diameter.

This cohesive force is a good model for capillary forces between beads with nanoasperities: capillary bridges are then located between two asperities belonging to two different beads or between one asperity of one bead and one relatively flat surface of the other bead. Therefore, the attractive force increases with an increasing amount of liquid rendering our spring model for a cohesive force relevant.

The discs are put in a shearing cell with blades, one can see an example of this shearing cell in figure 1. Periodic boundary conditions are imposed on the left and right hand sides of the cell. The shear cell is made of discs in order to simplify the interactions of the bulk discs and the shear cell: the upper cover is made of discs of non-zero effective mass (allowing the vertical movement of the cover) and the bottom of the cell is made of discs with zero effective mass (allowing a stable position of the shear cell with respect to gravity). Shear is applied on the discs by translating the upper cover at constant velocity, whatever the resistance to translation of the granular medium. The upper cover of the cell is allowed to undergo a vertical shift, the magnitude of this shift depending on the weight of this upper cover (and hence on the effective mass of the upper cover discs), on the velocity of the upper cover and on the disc assembly dilation.

3. Results and discussion

The parameters of our computations were the following: the velocity of the upper cover was $v = 0.2 \text{ mm s}^{-1}$ and the weight of the cover was equal to 0.552 g, the mass of one disc being equal to $2.76 \times 10^{-3} \text{ g}$. The length of the cell was $L = 8 \text{ mm}$ and the height of the blades was $h = 1 \text{ mm}$. We used $N = 720$ discs. The dissipation coefficient was equal to 0.7 m s^{-1} , the

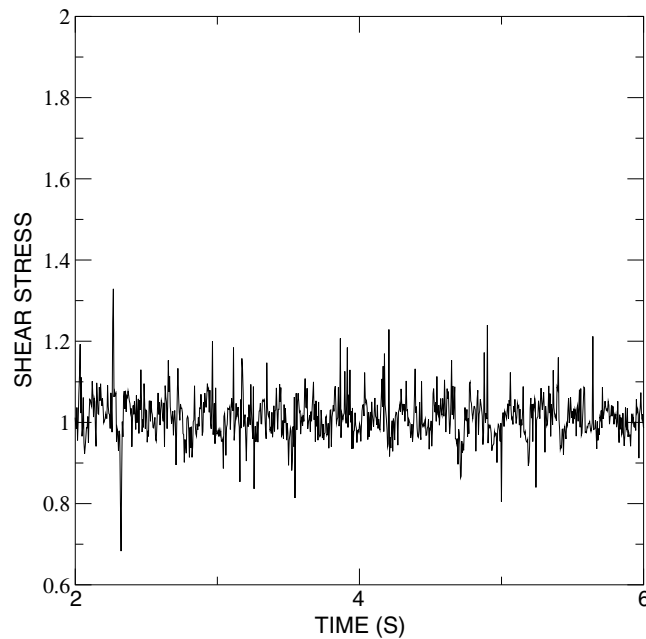


Figure 2. Stress signal (arbitrary units) as a function of time (in s for a shearing rate $v = 0.2 \text{ mm s}^{-1}$).

Young modulus was $Y = 2020 \text{ g m}^{-1} \text{ s}^{-2}$ and the spring constant was $K = 41.4 \text{ g m}^{-1} \text{ s}^{-2}$. Our model represents mesoscopic beads (i.e. larger than particles in a powder) with a very weak cohesive force, hence it is different from models with strong cohesion. The quantity of discs used here is sufficient to analyse their behaviour on a mesoscopic level.

We computed the total force acted on the upper cover by the disc assembly as a resistance to shear. For this, we added only the horizontal coordinates of the forces acting on the cover. This total force is similar to a stress.

In figure 2, one can see an example of the evolution of this total force as a function of time; in this case a non-periodic signal was found with the preceding parameters. The Fourier transform of this last signal is plotted in figure 3. The signal was saved only when the permanent regime was obtained, when the height of the cover and the mean signal were steady. This signal appears to be very noisy: experiments with a shearing cell with blades lead to similar irregular signals (see [18]).

In figure 4, one can see another example of the total force as a function of time when the signal is periodic: the shear rate is equal to $v = 16 \text{ mm s}^{-1}$ (other parameters were the same). The corresponding Fourier transform is plotted in figure 5: there appear peaks at regular intervals, which are the signature of a periodic signal. The corresponding characteristic frequency is equal to $f = 8 \text{ Hz}$.

Hence, the stress signal becomes periodic for shearing rates larger than 8 mm s^{-1} and up to 120 mm s^{-1} , from Fourier analysis of the stress signals corresponding to these shearing rates in our simulations.

In order to understand the origin of the intermittent signal, we made an analysis of the internal geometrical structure i.e. the locations of the discs during shearing in the cell.

In figure 6 one can see the density of discs as a function of the distance (in disc diameters) to the bottom of the cell. We computed this density for two shearing rates: $v = 0.2$ and

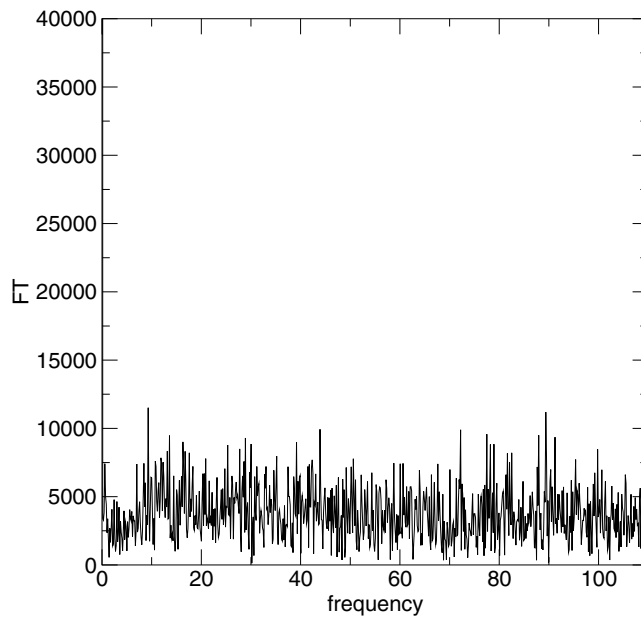


Figure 3. Fourier transform of the stress signal (arbitrary units) as a function of frequency (in Hz) for a shearing rate $v = 0.2 \text{ mm s}^{-1}$.

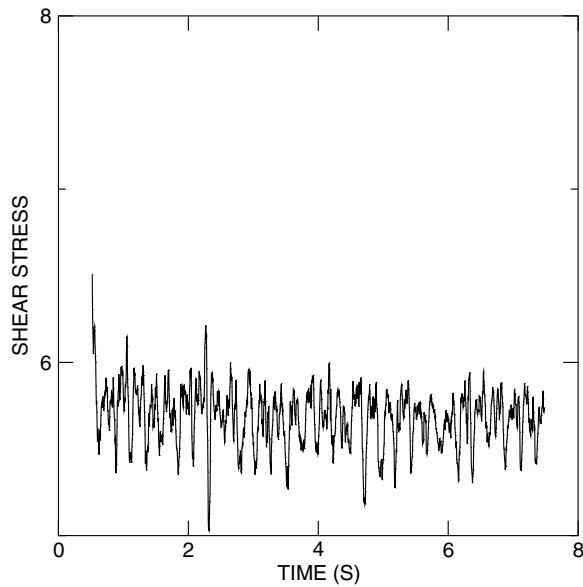


Figure 4. Stress signal (arbitrary units) as a function of time (in s) for a shearing rate $v = 16 \text{ mm s}^{-1}$.

120 mm s^{-1} . For $v = 0.2 \text{ mm s}^{-1}$, it appears that the discs have a two-dimensional crystalline structure: we observe periodic peaks in the density of discs. In the intervals between the peaks, the density increases slowly as a function of the distance to the bottom. All this means that the discs are structured in layers. For $v = 120 \text{ mm s}^{-1}$ this layered structure is also present

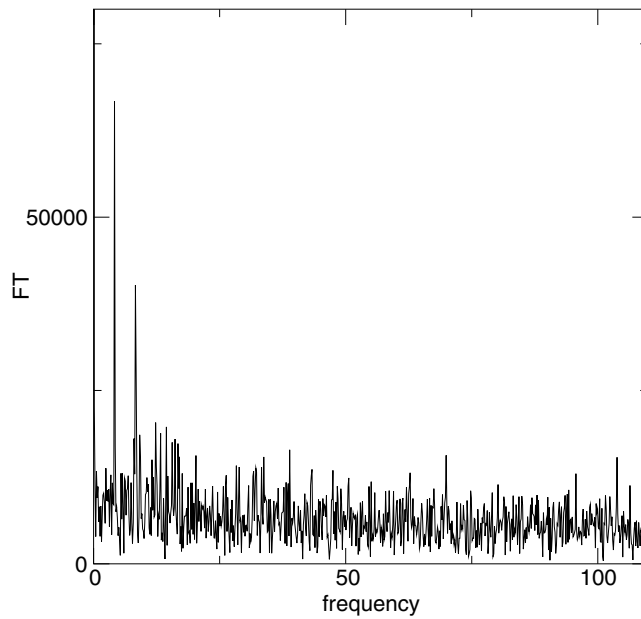


Figure 5. Fourier transform of the stress signal (arbitrary units) as a function of frequency (in Hz) for a shearing rate $v = 16 \text{ mm s}^{-1}$.

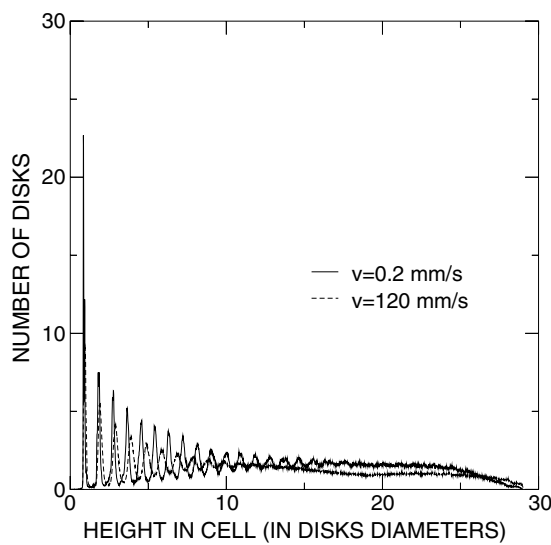


Figure 6. Horizontal disc densities as a function of the distance (in disc diameter units) to the bottom of the shearing cell, for two shearing velocities $v = 0.2 \text{ mm s}^{-1}$ (continuous line) and $v = 120 \text{ mm s}^{-1}$ (long dashed line).

but with lower densities (for each layer). For this high shearing rate the layered structure disappears at 11 disc diameters from the bottom, and from then on decreases slightly, while for the lower velocity the layered structure is maintained up to 16 disc diameters from the bottom, and decreases only at a distance to the top corresponding to the presence of the blades. These

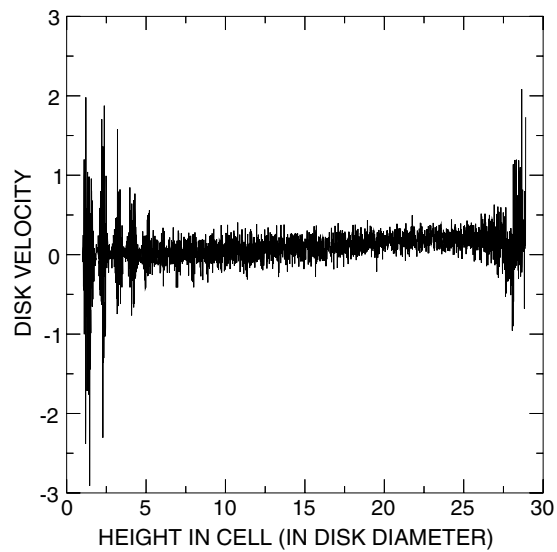


Figure 7. Horizontal velocities (in mm s^{-1}) of the discs as a function of the distance to the bottom of the cell (in disc diameter units) for a shearing rate $v = 0.2 \text{ mm s}^{-1}$.

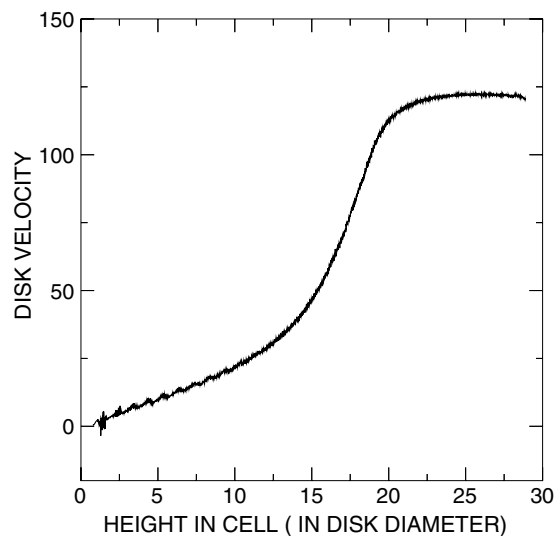


Figure 8. Velocities (in mm s^{-1}) of the discs as a function of the distance to the bottom of the cell (in disc diameter units) for a shearing rate $v = 120 \text{ mm s}^{-1}$.

layered structures are a consequence of the dimension of space: two dimensional. Indeed, the discs try to lower their resistance to shear and hence take place in a layered structure where the layers are parallel to the shearing force.

Let us compare the structure of the discs and the velocities of discs inside the cell. For this we took a snapshot of the instantaneous horizontal velocities of the discs at a given time t of the permanent regime. Figure 7 is this snapshot for a shearing rate $v = 0.2 \text{ mm s}^{-1}$ and figure 8 is the snapshot for a shearing rate $v = 120 \text{ mm s}^{-1}$.

Let us examine figure 7 in the light of figure 6. Both figures have been set up with a shearing rate $v = 0.2$ mm. In figure 7, one can see that there remains the layered structure of figure 6: close to the bottom of the cell (close to zero in disc diameters) the velocities of the discs are periodically high, for distances up to 5 disc diameters from the bottom. A shearing band does not appear clearly: the velocities of the discs increase slowly and regularly from abscissa 5 to abscissa 25. What is interesting to see is that the discs undergo negative and positive velocities, that means that the discs follow the shear direction and also the inverse direction. This happens near the bottom of the cell but also in the region of the blades. This is a consequence of the cohesion: when two discs collide, due to the spring linking them, these two discs undergo a periodic oscillation backward and forward. As all neighbouring discs are related by springs, there are collective oscillations of the discs inside one layer. These collective horizontal oscillations disappear when the layered structure disappears.

Now, let us look at figure 8. There are no more collective horizontal oscillations because of the high value of the shearing rate ($v = 120$ mm s⁻¹). A shearing band appears clearly where the velocities of the discs increase regularly from almost zero to the value of the shearing rate. This shearing band has a width of ten disc diameters.

The question remaining is whether there is here a stick–slip phenomenon with a constant shearing rate, i.e. a infinite shearing force. In the light of the results that we obtained we can say that the discs try to decrease their resistance to shear by arranging themselves in layered structures parallel to the shearing direction. Furthermore, due to the cohesion given by springs between very next neighbours, the discs undergo small oscillations, in the direction of the shear and in its inverse.

The discs interact by way of the springs. So, we may say that we have obtained a stick–slip phenomenon in an assembly of discs put in a two-dimensional shearing cell. The stress signal that we have obtained is the result of a sticking stage, when the springs linking our discs enlarge and the potential energy increases. The slip stages correspond to the periods where the springs relax and the potential energy is released.

This is a mean behaviour, and one cannot say whether all springs relax at the same times. From our Fourier analysis of the stress signal, we can say that for $v < 8$ mm s⁻¹ (no characteristic peak in the Fourier curve) the relaxing and enlarging of the springs are not correlated: the stress signal is non-periodic. Meanwhile, for 8 mm s⁻¹ $< v < 120$ mm s⁻¹ a characteristic peak appears in the Fourier signal, the relaxing and enlarging of the springs are correlated in time, and the stress signal is periodic.

We computed from these Fourier transforms the characteristic frequencies of the stick–slip signal for 8 mm s⁻¹ $< v < 120$ mm s⁻¹ and for simulation boxes of two sizes, as a function of the shearing rate. The dimensions of the first corresponds to the preceding computations, i.e. width 8 mm and height of the blades 1 mm with 720 discs. The dimensions of the second are width 12 mm and height of the blades 1.5 mm with 1080 discs. These larger dimensions have been chosen in order to get a number of discs small enough to avoid time consuming computations, but also in order to obtain significant differences between the two systems.

Results are shown in figure 9. We see in this figure that the stick–slip signal frequency depends on the dimensions of the simulation box. As we used springs to model cohesion in the bulk of our particles, we can say that the characteristic frequencies of the oscillations of the assembly of springs hence depend on the dimensions of the simulation box, like the frequency of a unique oscillator in a box of variable dimensions, even if we use periodic boundary conditions.

The characteristic frequencies also depend linearly on the shearing rate. This is the signature that the dissipation of energy as a function of time is small compared to the shearing rate: the amount of energy brought by the constant shearing rate counterbalances the loss of

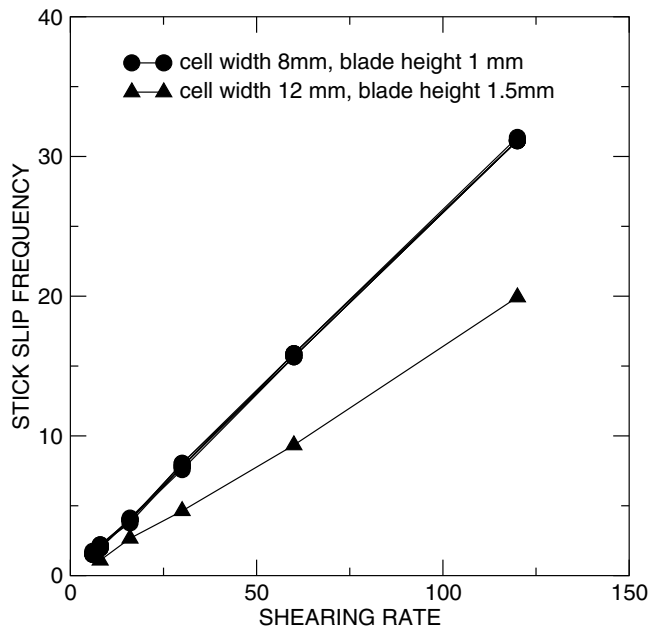


Figure 9. Characteristic frequencies of the stick–slip signal for two simulation box dimensions (width = 8 mm and height of blades = 1 mm with 720 discs; width = 12 mm and height of blades = 1.5 mm with 1080 discs), as a function of shearing rate.

energy due to dissipation when two particles overlap. Indeed, during each stick event, energy is accumulated by way of the elasticity of the discs and inside the springs (potential energy); as dissipation is counterbalanced by the energy brought by the constant shearing rate, the assembly of springs behaves as a unique spring with no dissipation. This unique spring will elongate until it reaches a given threshold length which depends on the maximum length for the individual springs representing capillary interactions between discs. So the whole assembly of discs can be modelled by this unique spring whose position can be easily calculated:

$$x(t) = \frac{v}{\omega} \sin(\omega t) \quad (5)$$

where $\omega = \sqrt{\frac{k}{M}}$ is the characteristic frequency of the stick–slip where M is the mass of the whole assembly of discs. We see that the position x of the assembly of discs represented by the unique spring depends linearly on the shear velocity v . So the threshold length will be reached in a time interval (i.e. a period) inversely proportional to v . Hence the frequency will increase linearly with the shear velocity v . Moreover, if the mass M of the whole assembly of discs increases, i.e. if the system containing the discs is larger with discs of the same diameter, the characteristic frequency decreases.

4. Conclusion

We computed the behaviour of two-dimensional discs with weak cohesion in a shearing cell with blades. Though the shearing rate is constant, we observe a typical stick–slip stress signal. As the cohesion is added by way of springs linking very next neighbouring discs, we can say that the stick stage corresponds to a collective enlargement of all springs where potential energy is

accumulated. The slip stage results from the relaxing of the springs. Our stress signal becomes periodic for shearing rates values larger than a given threshold. The characteristic frequencies of the stick–slip signal depend on the dimensions of the simulation box. As the cohesion between the particles has been modelled by springs, we can say that the whole assembly of interacting particles behave as a global unique spring. Hence each characteristic frequency depends on the shearing rate. Moreover, as the shearing rate is constant, the amount of energy necessary to counterbalance dissipation is always adequate, leading to a linear evolution of the frequencies with shearing rate.

References

- [1] Albert R, Albert I, Hornbaker D, Schiffer P and Barabasi A L 1997 *Phys. Rev. E* **56** R6271
- [2] Alonso J J, Hovi J P and Herrmann H J 1998 *Phys. Rev. E* **58** 672
- [3] Barabasi A L, Albert R and Schiffer P 1999 *Physica A* **266** 366
- [4] Bocquet L, Charlaix E, Ciliberto S and Crassous J 1998 *Nature* **396** 735
- [5] Fraysse N, Thome H and Petit L 1997 *Powder and Grains 1997* ed R P Behringer and J T Jenkins (Rotterdam: Balkema)
- [6] Fraysse N, Thome H and Petit L 1999 *Eur. Phys. J. B* **11** 615
- [7] Halsey T C and Levine A J 1998 *Phys. Rev. Lett.* **80** 3141
- [8] Hornbaker D J, Albert R, Albert I, Barabasi A L and Schiffer P 1997 *Nature* **387** 765
- [9] Mason T G, Levine A J, Ertas D and Halsey T C 1999 *Phys. Rev. E* **60** 50 44
- [10] Nase S T, Vargas W L, Abatan A A and McCarthy J J 2001 *Powder Technol.* **116** 214
- [11] Nedderman R M 1992 *Statics and Kinematics of Granular Materials* (Cambridge: Cambridge University Press)
- [12] Ristow G H 1994 Granular dynamics: a review about recent molecular dynamics simulations of granular materials *Annual Review of Computational Physics* vol 1, ed D Stauffer (Singapore: World Scientific) p 275
- [13] Ristow G H 1996 *Europhys. Lett.* **34** 263
- [14] Olivi-Tran N, Fraysse N, Girard P, Ramonda M and Chatain D 2002 *Eur. Phys. J. B* **25** 217
- [15] Olivi-Tran N, Pozo O and Fraysse N 2004 *Modell. Simul. Mater. Sci. Eng.* **12** 671
- [16] Restagno F, Bocquet L and Charlaix E 2004 *Eur. Phys. J. E* **14** 177
- [17] Samadani A and Kudrolli A 2000 *Phys. Rev. Lett.* **85** 5102
- [18] Pozo O, Fraysse N and Olivi-Tran N 2005 *Powder and Grains 2005* ed R Garca-Rojo, H J Herrmann and S McNamara (Rotterdam: Balkema)